inventions

MDPI

Article

Overcoming Chip Shortages: Low-Cost Open-Source Parametric 3-D Printable Solderless SOIC to DIP Breakout Adapters

Cameron K. Brooks [1], Jack E. Peplinski [2] and Joshua M. Pearce [1,2,*]

[1] Department of Electrical & Computer Engineering, Western University, London, ON N6A 5B9, Canada; cbrook49@uwo.ca
[2] Ivey Business School, Western University, London, ON N6A 5B9, Canada; jpeplin2@uwo.ca
* Correspondence: joshua.pearce@uwo.ca

Abstract: The COVID-19 pandemic exposed the vulnerability of global supply chains of many products. One area that requires improved supply chain resilience and that is of particular importance to electronic designers is the shortage of basic dual in-line package (DIP) electronic components commonly used for prototyping. This anecdotal observation was investigated as a case study of using additive manufacturing to enforce contact between premade, off-the-shelf conductors to allow for electrical continuity between two arbitrary points by examining data relating to the stock quantity of electronic components, extracted from Digi-Key Electronics. This study applies this concept using an open hardware approach for the design, testing, and use of a simple, parametric, 3-D printable invention that allows for small outline integrated circuit (SOIC) components to be used in DIP package circuits (i.e., breadboards, protoboards, etc.). The additive manufacture breakout board (AMBB) design was developed using two different open-source modelers, OpenSCAD and FreeCAD, to provide reliable and consistent electrical contact between the component and the rest of the circuit and was demonstrated with reusable 8-SOIC to DIP breakout adapters. The three-part design was optimized for manufacturing with RepRap-class fused filament 3-D printers, making the AMBB a prime candidate for use in distributed manufacturing models. The AMBB offers increased flexibility during circuit prototyping by allowing arbitrary connections between the component and prototyping interface as well as superior organization through the ability to color-code different component types. The cost of the AMBB is CAD $0.066/unit, which is a 94% saving compared to conventional PCB-based breakout boards. Use of the AMBB device can provide electronics designers with an increased selection of components for through-hole use by more than a factor of seven. Future development of AMBB devices to allow for low-cost conversion between arbitrary package types provides a path towards more accessible and inclusive electronics design as well as faster prototyping and technical innovation.

Keywords: 3D printing; additive manufacturing; breakout; chip shortage; design; electronics; innovation; open electronics; open hardware; open source; prototyping; solderless; SOIC

Citation: Brooks, C.K.; Peplinski, J.E.; Pearce, J.M. Overcoming Chip Shortages: Low-Cost Open-Source Parametric 3-D Printable Solderless SOIC to DIP Breakout Adapters. *Inventions* **2023**, *8*, 61. https://doi.org/10.3390/inventions8020061

Academic Editor: Craig E. Banks

Received: 23 March 2023
Revised: 5 April 2023
Accepted: 7 April 2023
Published: 10 April 2023

1. Introduction

The global economy has been structured by companies that rely largely on optimal structures of supply chains to achieve competitive advantages [1]. This model was recently challenged during the COVID-19 pandemic as it crippled the global economy [2]. Initially, the primary focus of supply chain disruptions was in the medical area [3]. As the entire global population appeared at risk, finding solutions to medical supply shortages was imperative, and a number of approaches surfaced, including: (i) low-tech solutions [4], (ii) open hardware [5] or open hardware design [6], and (iii) distributed manufacturing [7]. Some of these approaches, such as distributed manufacturing using 3-D printing to make life-saving supplies on demand, proved effective [8] and included personal protective equipment (PPE) [9] such as face shields [10,11], masks [12], N95 respirators [13], N95

mask adapters [14], heat-sterilizable masks [15], full face respirators [16], and powered air-purifying particulate respirators (PAPRs) [17]. In addition, this approach was effective at fabricating testing supplies and equipment such as nasopharyngeal swabs [18,19] and infrared thermometers [20]. Open hardware approaches were also used to make sterilization equipment [21,22], and even sophisticated electronics, needed for what appeared at the time to be a shortage of ventilators, proved possible in this model [23,24], as did units to test them [25,26].

As the pandemic continued, supply chain disruptions occurred in other sectors such as semiconductors [27] and electronics [28], causing a chip shortage that impacted everything from hand-held consumer goods [29] to the automobile industry [30]. The wake-up call from the pandemic [31] makes the value of having supply chain resilience clear in all areas [32]. One area with needed resilience of particular importance to those that prototype electronics equipment is that of the shortage of basic dual in-line package (DIP or DIL) electronic components packaging. DIP components are normally used on breadboards to prototype electronics before making a final copy or converting to a small outline integrated circuit (SOIC) to make surface-mounted integrated circuits. Prototyping with an SOIC is possible, but it is both physically challenging and time consuming compared to using a DIP. Another option for using non-DIP package components with breadboards and protoboards involve PCB breakout boards (BBs), but this incurs additional costs and requires soldering, which further increases cost and reduces reusability of components. During the pandemic, it anecdotally appeared that DIP chips were often in the shortest supply with the longest lead times; SOIC chips, although still in short supply, were more easily obtained because they are manufactured in higher volumes. To determine if this anecdotal lack of selection was an issue for electronic designers, data relating to the stock quantity and number of product offerings for a sample category were extracted for this study from the Digi-Key Electronics website.

The observed issue of a component having the desired function but not satisfying the physical constraints can apply to numerous electrical component types. Using additive manufacturing to create structures that incorporate conductors can be used to address this issue. To demonstrate proof-of-concept, off-the-shelf conductors and an open-source 3-D printer were used in an open hardware approach to overcome the anecdotal lack of DIP components in an application case study to evaluate the technical and economic feasibility of the proposed approach. This study summarizes the design, testing, and use of a simple, parametric, 3-D printable device that allows for SOIC-type components to be used in DIP package circuits (i.e., breadboards, protoboards, etc.). The geometry was designed to (1) enforce physical contact between component leads and header pins and (2) guide header pins to align and make contact with the breadboard or protoboard. The design was developed to provide reliable and consistent electrical contact between the component and the rest of the circuit and was demonstrated with reusable 8-SOIC to DIP breakout adapters and a simple circuit involving common components. The results are presented in the context of a concept that can be further expanded to other surface-mount and through-hole component packages. The manufacturing time and costs are discussed along with the possibility of eliminating the need for DIP in the future. It should be noted that although a specific geometry for a specific use case, in this case, 8-SOIC to DIP, is presented, this concept could be applied in many ways. Using 3-D printed geometry to enforce electrical contact between conductors can be achieved in more than one fashion and could be applied in several different contexts, including breakout boards, connectors, and other electromechanical devices.

There are existing approaches that use additive manufacturing to create conductive structures. Some of these methods include direct printing of circuits using conductive thermoplastic filament [33–35], usage of conductive liquids or epoxies that are added to two- or three-dimensional substrates using micro dispensing, spraying, or other post-processing techniques to create traces [36–38], metal 3-D printing technologies such as selective laser sintering that can additively manufacture precise and complex circuits [39,40], and the

usage of stereolithography-based techniques [41,42]. The approach presented here is distinct from all of this previous work due to its simplicity and accessibility as it can be created using virtually any modern desktop fused filament fabrication (FFF) 3-D printer and leverages off-the-shelf conductors.

2. Materials and Methods

To display the need for the presented AMBB in this application case, the data for similar devices relating to component package and stock quantity were extracted from the Digi-Key Electronics website. DigiKey.ca was chosen, as it is the 5th largest electronic component distributor in North America and the 7th largest worldwide as of 2016 [43]; furthermore, the components used to test the AMBB were sourced from DigiKey.ca. The data were extracted from product pages from the "Embedded Microcontrollers" section [44]. An open-source website scraper was written in Python and run locally on a laptop at 8 PM MST on 3 July 2022. Two software packages were used: Selenium [45] and Beautiful Soup [46]. Selenium was used to automate the browser clicking through each page and Beautiful Soup was used to get the data from each page. The data from each page were then written to a CSV file. The category listed 74,729 items, and the CSV file contained the same number of items, indicating a successful and comprehensive scrape. Resulting data was categorized by mounting type: "Through Hole" as through-hole, "Surface Mount" and "Surface Mount, Wettable Flank" as surface mount, and all unspecified or other mounting types as neither/unspecified. The data was processed and interpreted in three different ways: (1) summing the stock numbers for the three defined categories, (2) summing the number of component offerings for the three defined categories, and (3) summing the number of component offerings with non-zero stock for the three defined categories. These three categories were then summed together to ensure no data were omitted. The resulting data were then converted to percentages.

The development of the device for the presented application case was centered on six design goals: (1) to create a 3-D printable geometry that would provide reliable electrical contact between 8-SOIC components and a standard DIP-sized breadboard or protoboard; (2) complete reusability of the SOIC component and printed device; (3) complete design parameterization; (4) usage of off-the-shelf materials; (5) minimization of device footprint; (6) optimization for use across RepRap class [47–49] fused filament fabrication-based 3-D printers of varying tolerances and capabilities. This section will examine the design decisions in the context of these six design goals as well as the equipment, software, and materials involved in the design, manufacture, and validation of the proposed design.

OpenSCAD, an open-source script-only based modeler [50], and FreeCAD, an open-source parametric 3-D modeler [51], were both used for the computer-aided design (CAD) of the additive manufacture breakout board (AMBB). The models from both OpenSCAD and FreeCAD were functionally identical and were both created to provide users with more flexibility and increase accessibility. The AMBB consisted of three main parts: the main enclosure, the component housing, and the securing bolt seen in Figure 1. The enclosure had six main features: (1) a cavity to hold the component housing, (2) a threaded hole for the securing bolt, (3) eight angled channels to guide and secure the header pins, (4) two large symmetrically placed pockets that penetrate into the main cavity from above, (5) two small symmetrically placed slots that penetrate into the main cavity from below, and (6) a track that runs along the main cavity floor and exits through the back wall. The component housing had two main features: a cavity to hold and secure the component and two rows of symmetrically placed slots. The bolt was parametrically linked to the enclosure such that the threaded portion of the bolt was a solid inversion of the threaded hole that extended into the cavity from the top of enclosure. The bolt on the AMBB shown included a radius tolerance of 0.95, resulting in the radius of the bolt being 0.10 mm smaller than that of the receiving hole. Modification of the bolt and threading sizes may be required when different devices and materials are used for manufacturing; this can be easily done by modifying the four bolt tolerance parameters in the OpenSCAD model (bolt_rad_tol, threading_pitch_tol,

thread_height_to, and thread_depth_tol) or manually changing the desired dimensions in the FreeCAD model. The two large symmetrically placed pockets on the enclosure and the two symmetrically placed pockets on the component housing function to accommodate multi-meter probes for checking electrical contact between component leads and header pins. The two small symmetrically placed slots on the enclosure function to reduce printing artifact at the end of the channels and allow for visual confirmation of the header pin placement within the channels.

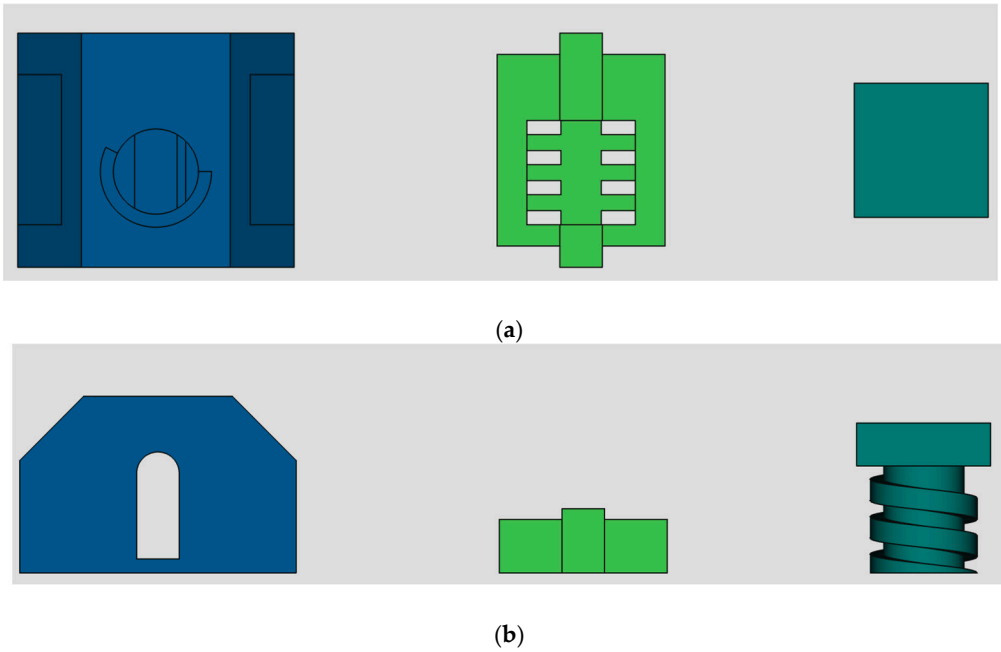

Figure 1. FreeCAD view of the enclosure (**left**), component housing (**center**), and securing bolt (**right**); (**a**) top view; (**b**) rear view.

The AMBB was manufactured using fused filament fabrication (FFF) technology on an unmodified open-source Original Prusa i3 MK3S+ [52] with a 1.75 mm Prusament brand polylactic acid (PLA) filament on a double-sided textured PEI powder-coated spring steel sheet using a 0.40 mm factory nozzle. The model was exported from FreeCAD as an STL file; then, the G-code was generated and exported to an SD card using PrusaSlicer 2.4.2 software [53]. Layer height was set to 0.10 mm, default brim was active, thin-wall detection was turned on, and infill was set at 15%; the temperatures were set based on the Prusament PLA preset included as part of Prusaslicer: 215 °C for the nozzle (all layers) and 60 °C for the bed (all layers). Detailed printer and slicer settings are both located in the associated Open Science Framework repository [54]. The first layer was printed at 50% speed, which then remained at 100% for the remainder of the print.

Once the printing process was complete, the three parts were removed from the print bed; other excess plastic artifacts were removed using needle nose pliers and ESD-11 tweezers. Right-angle male header pins (7.5 × 13.0 × 0.5 mm) were then inserted into the enclosure channels; the use of pliers can be helpful, especially if there are 3-D printing artifacts in the channel. Care must be taken when inserting the header pins, since over-insertion of the header pin may damage the terminal face of the channel, causing the header pin to sit incorrectly. The component was then inserted into the component housing cavity, and both inserted into the main cavity of the enclosure; the component housing was pressed flush with the front face of the enclosure; then, the bolt was screwed into the threaded hole on the enclosure and adequately tightened.

The completed AMBB was tested with an AN8205C portable multi-meter using the continuity function to confirm a short-circuit between each of the component leads and their respective header pins. To demonstrate the versatility of the AMBB, an inverting

amplifier circuit was constructed using an 8-SOIC OP07DDR operational amplifier. The schematic with nominal source and component values can be seen in Figure 2. OP07DDR was supplied by generic 9 V batteries, and the input signal was supplied by a 3.3 V voltage source from an Arduino Uno REV3.

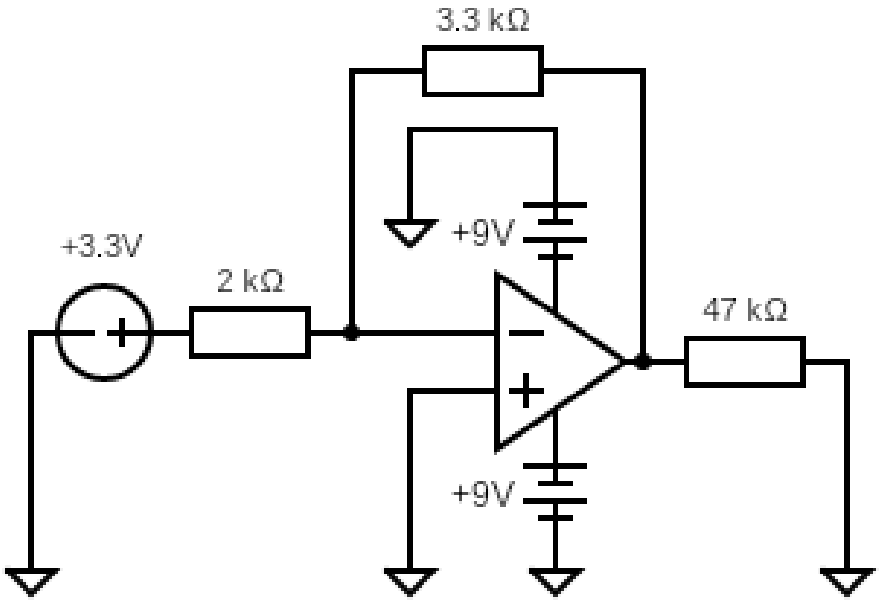

Figure 2. Test circuit schematic for an inverting amplifier with a nominal 3.3 V input signal and supplied with nominal 9 V batteries.

Finally, an economic analysis was carried out to determine the cost difference associated with using AMBBs for electronics prototyping versus that of traditional methods. First, a per-unit cost for using an AMBB and using a traditional PCB-based BB was estimated. All dollar amounts presented in this paper are in CAD. The per-unit cost of the AMBB was calculated from the mass of PLA used, quantity of header pins used, and energy consumed by the printer. The filament cost (C_{PLA}) is given by Equation (1) using the mass of PLA to print a full sheet, as given by PrusaSlicer ($m_{PLA,fs}$), 102.30 g; the number of complete AMBBs that includes all three components on a full sheet (n_{fs}), 97; the cost for one spool of Prusament brand polylactic acid (PLA) filament ($C_{PLA,\ spool}$), 38.94 CAD; and the mass of one PLA spool ($m_{PLA,spool}$), 1000 g:

$$C_{PLA} = \frac{m_{PLA,fs}}{n_{fs}} \frac{C_{PLA,spool}}{m_{PLA,spool}} \tag{1}$$

The cost of the header pins (C_{HPins}) used is given by Equation (2) using the cost for a package of right-angled header pins from Viinko Electronics HK ($C_{HPins,pkg}$), 1.16 CAD; the number of pins in the package ($n_{HPins,pkg}$), 400; and the required number of header pins for each AMBB ($n_{HPins,used}$), 8:

$$C_{HPins} = \frac{C_{HPins,pkg}}{n_{HPins,pkg}} n_{HPins,used} \tag{2}$$

The cost of the energy consumed ($C_{Energy,1}$) to print the device is given by Equation (3) using the average power consumption for printing generic PLA on an Original Prusa, when operated at an ambient temperature of 26 °C (room temperature), according to Prusa Research ($P_{Avg,PLA}$), 80 W; the print time for a full sheet ($t_{print,fs}$), 33.00 h (118,800 s); the

energy cost during off-peak times at the time of testing according to London Hydro [55] ($C_{London,op}$), 0.0812 CAD/kWh:

$$C_{Energy,1} = \frac{P_{Avg,PLA} \times t_{print,fs}}{n_{fs}} \frac{C_{London,op}}{1\,\text{kWh}} \frac{1\,\text{kWh}}{3.6E6J} \tag{3}$$

The per-unit cost of the PCB-based BB ($C_{BB,PCB}$) is given by Equation (4) using the cost of a PCB-base breakout board (BB) package ($C_{BB,pkg}$), 4.83 CAD; and the number of BBs per package ($n_{BB,pkg}$), 4:

$$C_{BB,PCB} = \frac{C_{BB,pkg}}{n_{BB,pkg}} \tag{4}$$

The cost of the solder (C_{solder}) used is given by Equation (5) using the estimated mass of solder required to attach the component and header pins to the PCB ($m_{solder,used}$), 0.2 g; the cost for generic 63–37 tin-lead solder wire ($C_{solder,pkg}$), 11.99 CAD; and the mass of the solder spool from Amazon.ca ($m_{solder,pkg}$), 50 g:

$$C_{solder} = m_{solder} \frac{C_{solder,pkg}}{m_{solder,pkg}} \tag{5}$$

The cost of the energy consumed to solder the component and header pins ($C_{Energy,2}$) is given by Equation (6) using an estimate for the power required for an experienced user to solder all joints for the pins and leads using a generic soldering iron ($P_{Avg,iron}$), 80 W; the time required to solder all joints for the pins and leads, assuming a warmup time of 30 s, ($t_{tot,iron}$), 200 s:

$$C_{Energy,2} = P_{Avg,iron} \times t_{tot,iron} \frac{C_{London,op}}{1\text{kWh}} \frac{1\text{kWh}}{3.6E6J} \tag{6}$$

All prices stated are based on the lowest-cost available generic version of the given product as of July 2022 in Ontario, Canada. The stated prices, quantities, and values may vary with time period, geographical location, availability, and user ability. The percentage savings of using an AMBB versus a traditional PCB-based breakout board is given by Equation (7).

$$\%Savings = \frac{C_{Total,PCB-BB} - C_{Total,AMCB}}{C_{Total,PCB-BB}} 100\% \tag{7}$$

3. Results

First, as can be seen by the results of the evaluation of the DigiKey website in both the quantity in Figure 3 and number in Figure 4, it is clear that there was far more selection for designers when surface-mount components could be used in place of through-hole components. As of 3 June 2022, only 12% of the electronics actually available (in stock) were through-hole, as shown in Figure 5.

The correct view of anecdotal limitations of using through-hole electronic components is clear. The results of the data scrape conducted for the "Embedded Microcontrollers" category on DigiKey.ca revealed that 94% of stock was SMD package components, 91% of product offerings were SMD package components, and 88% of in-stock product offerings were SMD package components. These results clearly demonstrate the increased selection of components available to electronics designers when given the ability to prototype with SMD package components, something which the AMBB has demonstrated as a key benefit. See the Open Science Framework repository for the spreadsheet containing the complete dataset and interpretation.

To give electronics designers access to SMD components without losing the ease of prototyping with through-hole components, all three components of the presented AMBB design were printed over 25 times in batch sizes ranging from 1 to 10 devices per print with a perfect success rate when the default brim setting was used. This demonstrated the proposed designs' viability for 3-D printing applications, making it a prime candidate for

use in a distributed manufacturing model [56], allowing for easy adoption by electronic designers. As an example, the AMBB design is shown in use with a constructed circuit in Figure 6 based on the design shown in Figure 2. The AMBB with the SMD chip works identically to a through-hole component.

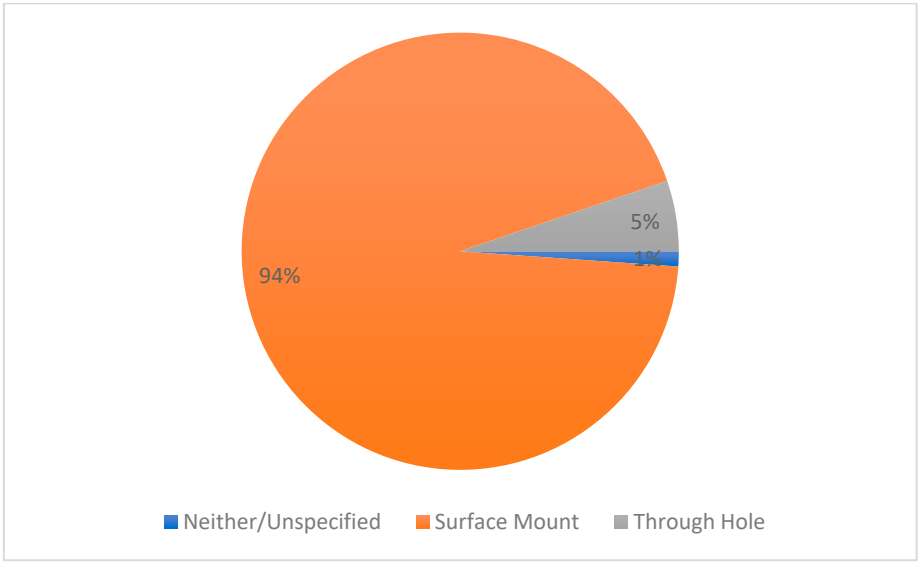

Figure 3. Quantity of surface-mount versus through-hole components.

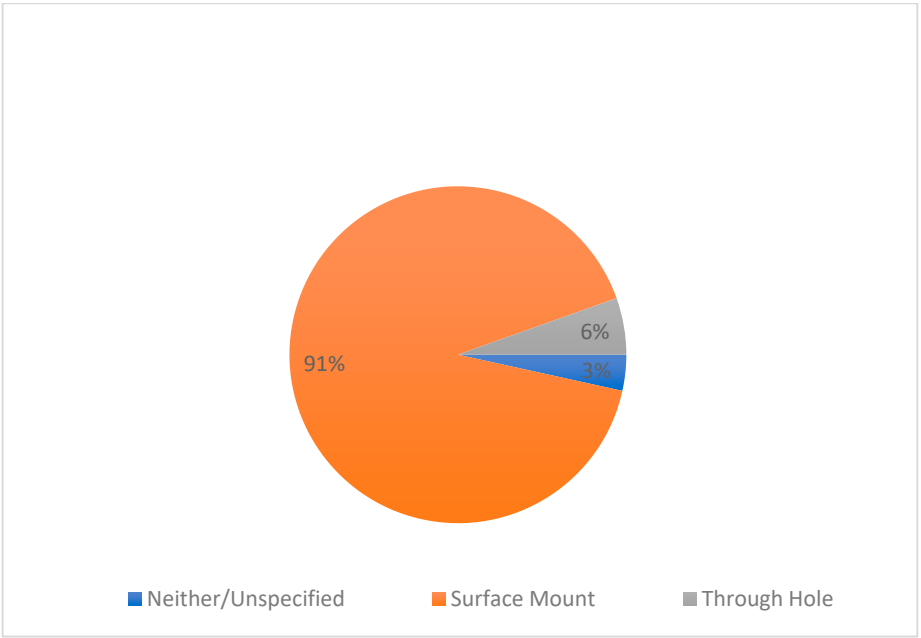

Figure 4. Number of surface-mount versus through-hole component product offerings.

The AMBB design allows for a huge amount of flexibility during circuit prototyping due to the ability for the user to use various connection methods. The AMBB can be used conventionally by directly inserting into the breadboard, as shown in Figure 6. The header pins can also instead be replaced by standard square terminal jumper wires, allowing for a connection at arbitrary points in the circuit while the AMBB rests on or beside the prototyping board in what is commonly referred to as the "dead bug configuration". Another similar configuration involves the header pins being flipped such that they are directed upwards, allowing for female-to-female or female-to-male jumper wires to be connected and then placed at arbitrary points in a circuit. Any of the mentioned configurations can

be used in combination depending on the users' goals. For example, the AMBB can be inserted into the breadboard; then, two of the header pins can be switched out for jumper wires to allow for direct connection to supplies, other breadboards, etc. Another useful advantage is the ability to use differently colored filaments, all with roughly equivalent mechanical properties [57], to color-code different components.

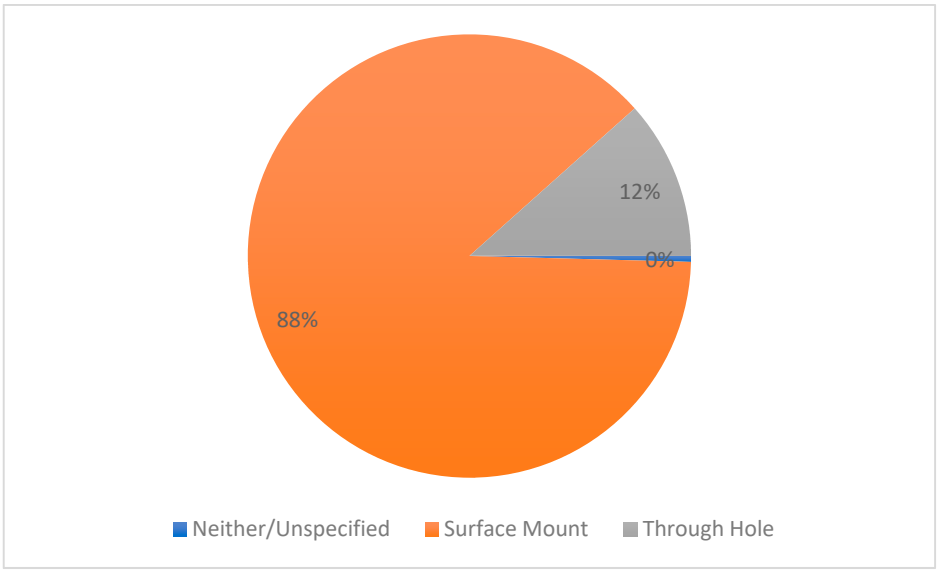

Figure 5. Number of surface mount versus through-hole components in stock product offerings.

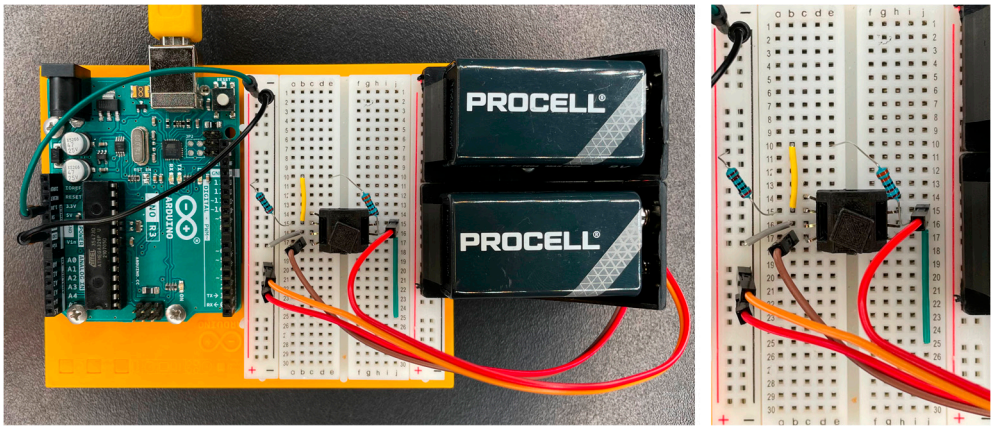

(**a**) (**b**)

Figure 6. (**a**) Constructed inverting amplifier circuit. (**b**) Close view of design used on a breadboard. This is a direct implementation of Figure 2, where 9 V are the batteries, the black AMBB contains an 8-SOIC op amp, and the 3.3 V is supplied using an Arduino UNO r3.

Table 1 displays the measured voltages from the constructed circuit shown in Figure 7. The theoretical value for the output signal presented in Table 1 was calculated using Equation (8); this equation assumes ideal behavior as pertains to the operational amplifier. In relation to Figure 6: R_{fb} = 3.3 kΩ, R_{input} = 2 kΩ, and V_{input} = +3.3 V; this gives V_{out} = −5.5 V as seen in Table 1, where R is resistance and V is voltage.

$$V_{out} = \frac{-R_{fb}}{R_{input}} V_{input} \tag{8}$$

Table 1. Experimental validation of AMBB demonstration circuit.

Description	Theoretical Value (V)	Value (V)
Input signal	+3.3	+3.41
Positive rail	+9.0	+8.96
Negative rail	−9.0	−8.28
Output signal	−5.5	−5.51

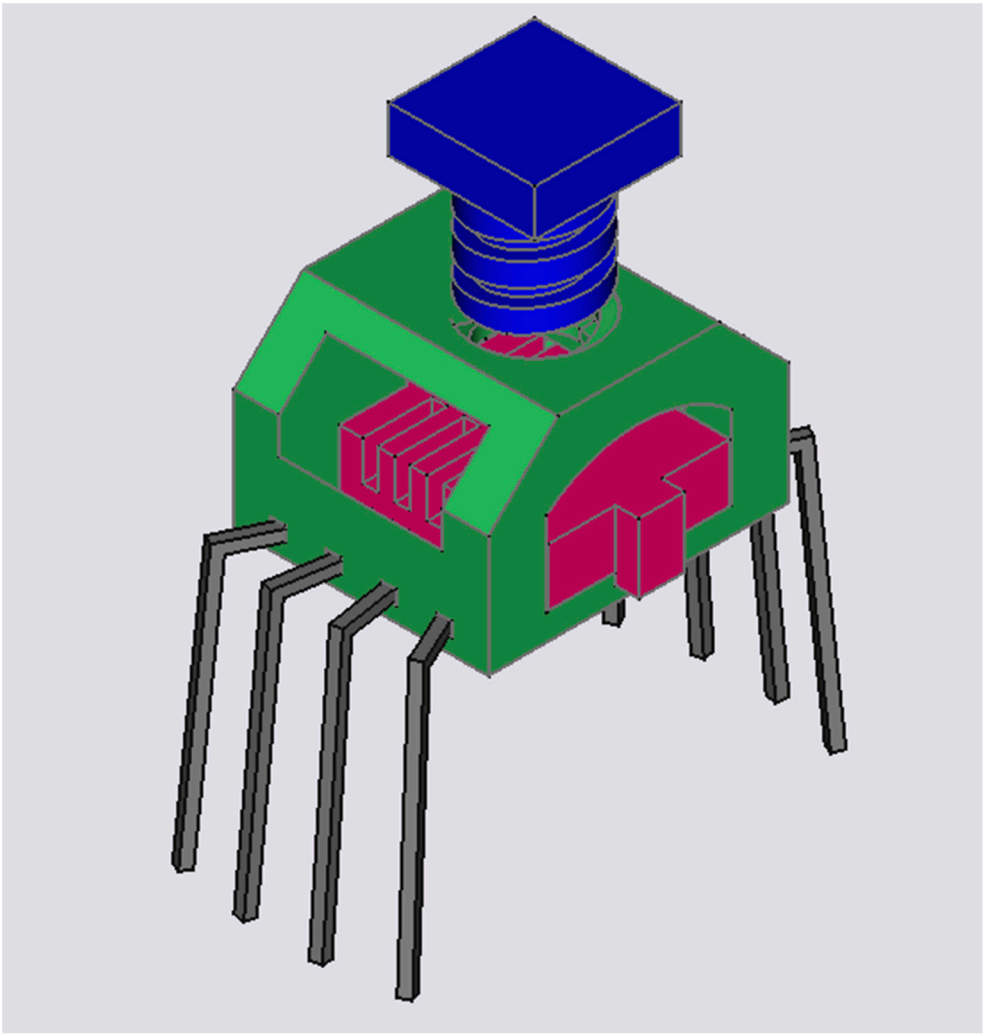

Figure 7. Orthographic view of the assembled CAD for the device.

Ultimately, all six of the design goals were satisfied. Design goal 1 was satisfied based on the successful continuity testing and constructed test circuit (Figure 2). Goal 2 was satisfied as none of the components nor the printed structures were damaged or altered from the components being inserted, tested, and removed from the AMBB. Goal 3 was successfully addressed as both the FreeCAD and OpenSCAD embodiments were designed to be parametrically linked such that users could alter individual parameters without having to then adjust the related geometry. Certain parameters are not fully parametric due to geometric complexity and may require manual adjustment; this includes pin access hole depth (PA_depth; OpenSCAD) and occasional re-selection of sketch support faces (multiple parameters; FreeCAD). The only two materials used were angled male header pins and PLA filament, which satisfies goal 4, since both can be purchased off the shelf from many suppliers. The footprint of the AMBB was 13 × 12 mm, which allowed for the placement of 15 AMBBs on a standard breadboard with a length of 63 pins. Moreover, the

height provided by the header pins allows for components and/or wires to be placed below the AMBB, which further minimized the devices' footprint. Together, this satisfies design goal 5 relating to minimizing the device footprint. The design did not: (1) include any functional structures with dimensions smaller than 0.4 mm, the standard FFF-based 3-D printer nozzle size, (2) require specialty filaments, or (3) require multi-material extrusion, which satisfies design goal 6 relating to optimization for use in various RepRap-class FFF-based 3-D printers. An assembly of the described device is shown in Figure 7, and a partial assembly displaying the internal geometry is shown in Figure 8.

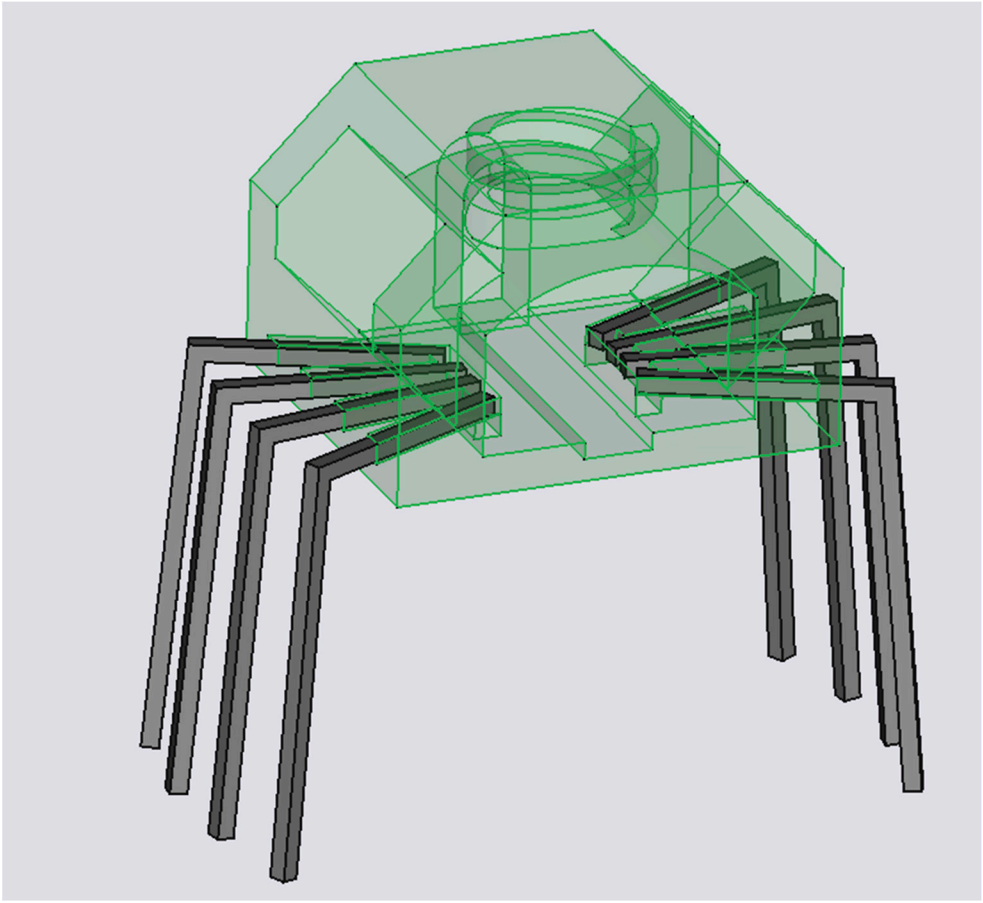

Figure 8. Partially assembled CAD for the device with a semi-translucent enclosure part.

Based on the sum Equations (1)–(3) using the corresponding values, the cost of the AMBB when printed as part of a full sheet was calculated to be 0.066 CAD/unit; the cost of contribution for the total AMBB cost was as follows: header pins 35%, PLA 62%, utility power 3%. Based on the sums of Equations (2) and (4)–(6) using the corresponding values, the cost of the conventional PCB-based breakout board was calculated to be 1.37 CAD/unit. According to Equation (7), the presented additive manufacturing-based breakout board design provided savings of over 94% when compared to a conventional PCB-based breakout board.

The proposed approach and overarching concept in this paper was successfully implemented for the presented application case and was shown to be both technical and economically feasible.

4. Discussion

A key design choice was the selection of materials, those being the male header pins as the electrical bridge between the breadboard and component terminals and the use of PLA as the print material. Header pins were used due to their availability, known

electrical properties, and frequent use in electronic prototyping. Header pins were chosen over solid high-gauge wire due to their rigidity, which translated to increased durability and hence reusability; furthermore, right-angled pins were selected over straight pins since forming the straight pins to the desired shape added labor time, damaged print on occasion, and decreased uniformity as well as reproducibility. PLA was chosen as the print material for several reasons: (1) it is electrically insulative, (2) widely available as one of the most common filament types, (3) it is offered in various colors, allowing for color coding of different components, and (4) increases sustainability due to the ability for it to be recycled in a distributed-recycling and additive-manufacturing (DRAM) context using either recyclebot [58] or direct extrusion [59] approaches. Although PLA can be recycled five times without losing appreciable mechanical strength [60], the biopolymer, often derived from corn, can be composted to help contribute to a sustainable circular economy [61]. With minimal alterations, however, other 3-D printing polymers could be used for this application. This includes recycled waste plastic from more common plastics such as acrylonitrile butadiene styrene (ABS). This, coupled with solar-powered 3-D printers [62–65] to cut electrical costs, would largely eliminate the 3-D printing material costs [66] and thus decrease the costs by over 60%. Even without these measures, by using only off-the-shelf parts, the open source AMBB system will save designers over 94% while increasing their selection of components for through-hole use by more than a factor of seven. This approach will radically reduce the time for prototyping. It should be pointed out that the time and economic savings from soldering surface mount chips was not included in the analysis, so all economic values can be considered extremely conservative. If this approach becomes widespread, it may provide a path to the elimination of DIP and other large outline package types as they are unnecessary, assuming that an AMBB is tailored to every chip.

Although this design has many advantages for electrical prototyping, it also has certain limitations. For example, the geometry of this model is such that the header pins are angled towards the pins of the IC. This limits scalability, since the addition of more pins will require that the outmost pins are either set at an increasingly greater angle and/or demand a longer channel distance. This will mean that a maximum number of pins will be reached for the current design either due to angular limitation or the channel length exceeding that of the header pins available. In this case, 0.4 mm was the width, 1.27 mm was the pitch of the SOIC terminals, and the 0.64 $\times$ 7.25 mm rectangles were the angled portion of the header pins that were vertically separated at the other end by 2.54 mm (the pitch of DIP terminals). If one could find sufficiently long pins, the practical maximum for conversion between these specific types (SOIC to DIP) would be 6 $\times$ 2 = 12 per side (24 for a two-sided chip as seen in Figure 9). Note that the image in Figure 9 is 1/4 since it was reflected over the x-axis and then the y-axis. It should also be noted that these were average values, since dimensions and tolerances vary slightly between different header pin and chip manufacturers. This limitation could be overcome by altering the current geometry or taking a modified approach to enforce electrical contact. This reveals a strong need for a software-based tool to generate arbitrary 3-D geometry to accommodate conductors and enforce contact based on a number of input parameters and constraints.

This leads to perhaps the most important and exciting aspect of the presented design: the direction that future work will take. The development of software that allows for quick and user-friendly generation of AMBB designs and other 3-D printed polymer-conductor arrangements, either as direct 3-D models or indirectly as scripts for use in OpenSCAD or similar design environments, would enable designers to have an unprecedented amount of flexibility and design freedom. This would essentially remove all constraints with respect to the availability of different component packages and connection types. This flexibility has value for those prototyping electronics of any kind [67], but most clearly for those developing open scientific hardware [68,69] and those working in low-resource settings [70]. For example, it is usually the case that the same component is available in various different package types, and it may be that stock and lead times vary; having a software-based tool to

generate AMBBs and other conductive geometries that convert between arbitrary package and connection types would allow the designer to purchase based on availability, lead time, or price rather than being limited to a certain package type. Additionally, this concept and approach can apply beyond adapting integrated circuit (IC) chips to be used for other electrical connection formats. Other useful future work may involve the investigation of different materials and geometric configurations that aim to reduce size, complexity, cost, and labor time to construct the AMBB and other conductive geometries. Finally, it should be mentioned that it could be further explored how this technique can be incorporated into or used in conjunction with existing techniques for additive manufacturing.

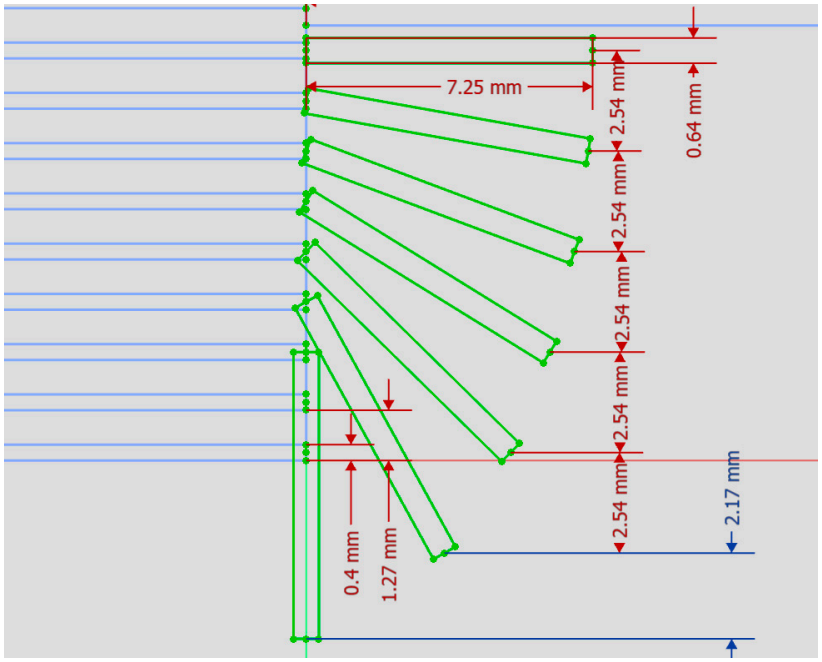

Figure 9. Geometric limitation of the AMBB approach.

5. Conclusions

This study has successfully demonstrated and validated an open source 3-D printable design that can convert 8-SOIC to DIP in a case study to evaluate the feasibility of the proposed concept and approach. The parametric design was created using two different open-source modelers, OpenSCAD and FreeCAD, both of which enable and encourage user modification and improvement. The three-part, two-material design was optimized for manufacturing with RepRap-class FFF-based 3-D printers, making the AMBB a prime candidate for use in a distributed manufacturing model. The AMBB offered increased flexibility during circuit prototyping by allowing an arbitrary connection between the component and prototyping interface as well as superior organization through the ability to color-code different component types. The cost of the 3-D printable AMBB was calculated to be 0.066 CAD/unit, which represents over 94% economic savings compared to the conventional PCB-based breakout boards. The AMBB successfully enables circuit designers to prototype with surface-mounted chips with the same ease that they are accustomed to with DIP chips. Extending this concept to other use cases and electrical connection types could increase prototyping flexibility and accelerate the rate of technological progress, particularly in low-resource facilities.

Author Contributions: Conceptualization, C.K.B. and J.M.P.; methodology, C.K.B. and J.M.P.; software, J.E.P.; validation, C.K.B.; formal analysis, C.K.B.; investigation, C.K.B.; resources, C.K.B. and J.M.P.; data curation, J.E.P. and C.K.B.; writing—original draft preparation, J.M.P. and C.K.B.; writing—review and editing, J.M.P., C.K.B. and J.E.P.; visualization, C.K.B.; supervision, J.M.P.; project administration, J.M.P.; funding acquisition, J.M.P. All authors have read and agreed to the published version of the manuscript.

Funding: This research was funded by the Natural Sciences and Engineering Research Council of Canada and the Thompson Endowment.

Data Availability Statement: All supplemental materials including open-source designs, data, and software are available on the Open Science Framework https://osf.io/dh6uy/ (accessed on 7 April 2023).

Acknowledgments: The authors would also like to thank Eugen J. Porter for helpful and insightful discussions.

Conflicts of Interest: The authors declare no conflict of interest.

References

1. Helmold, M.; Yılmaz, A.K.; Dathe, T.; Flouris, T.G. Global Supply Chains. In *Supply Chain Risk Management: Cases and Industry Insights*; Helmold, M., Yılmaz, A.K., Dathe, T., Flouris, T.G., Eds.; Springer International Publishing: Cham, Switzerland, 2022; pp. 79–89. [CrossRef]
2. Yu, Z.; Razzaq, A.; Rehman, A.; Shah, A.; Jameel, K.; Mor, R.S. Disruption in global supply chain and socio-economic shocks: A lesson from COVID-19 for sustainable production and consumption. *Oper. Manag. Res.* **2021**, *15*, 233–248. [CrossRef]
3. Bhaskar, S.; Tan, J.; Bogers, M.L.A.M.; Minssen, T.; Badaruddin, H.; Israeli-Korn, S.; Chesbrough, H. At the Epicenter of COVID-19–the Tragic Failure of the Global Supply Chain for Medical Supplies. *Front. Public Health* **2020**, *8*, 562882. [CrossRef] [PubMed]
4. Armani, A.M.; Hurt, D.E.; Hwang, D.; McCarthy, M.C.; Scholtz, A. Low-tech solutions for the COVID-19 supply chain crisis. *Nat. Rev. Mater.* **2020**, *5*, 403–406. [CrossRef] [PubMed]
5. Chagas, A.M.; Molloy, J.C.; Prieto-Godino, L.L.; Baden, T. Leveraging open hardware to alleviate the burden of COVID-19 on global health systems. *PLoS Biol.* **2020**, *18*, e3000730. [CrossRef]
6. Stirling, J.; Bowman, R. The COVID-19 Pandemic Highlights the Need for Open Design Not Just Open Hardware. *Des. J.* **2021**, *24*, 299–314. [CrossRef]
7. Pearce, J.M. Distributed Manufacturing of Open Source Medical Hardware for Pandemics. *J. Manuf. Mater. Process.* **2020**, *4*, 49. [CrossRef]
8. Saripalle, S.; Maker, H.; Bush, A.; Lundman, N. 3D printing for disaster preparedness: Making life-saving supplies on-site, on-demand, on-time. In Proceedings of the 2016 IEEE Global Humanitarian Technology Conference (GHTC), Seattle, WA, USA, 13–16 October 2016; pp. 205–208. [CrossRef]
9. Jafferson, J.; Pattanashetti, S. Use of 3D printing in production of personal protective equipment (PPE)—A review. *Mater. Today Proc.* **2021**, *46*, 1247–1260. [CrossRef]
10. Flanagan, S.T.; Ballard, D.H. 3D Printed Face Shields: A Community Response to the COVID-19 Global Pandemic. *Acad. Radiol.* **2020**, *27*, 905–906. [CrossRef]
11. Novak, J.I.; Loy, J. A quantitative analysis of 3D printed face shields and masks during COVID-19. *Emerald Open Res.* **2020**, *2*, 42. [CrossRef]
12. Vaňková, E.; Kašparová, P.; Khun, J.; Machková, A.; Julák, J.; Sláma, M.; Hodek, J.; Ulrychová, L.; Weber, J.; Obrová, K.; et al. Polylactic acid as a suitable material for 3D printing of protective masks in times of COVID-19 pandemic. *PeerJ* **2020**, *8*, e10259. [CrossRef]
13. Ballard, D.H.; Jammalamadaka, U.; Meacham, K.W.; Hoegger, M.J.; Burke, B.A.; Morris, J.A.; Scott, A.R.; O'Connor, Z.; Gan, C.; Hu, J.; et al. Quantitative Fit Tested N95 Respirator-Alternatives Generated With CT Imaging and 3D Printing: A Response to Potential Shortages During the COVID-19 Pandemic. *Acad. Radiol.* **2020**, *28*, 158–165. [CrossRef] [PubMed]
14. Imbrie-Moore, A.; Park, M.; Zhu, Y.; Paulsen, M.; Wang, H.; Woo, Y. Quadrupling the N95 Supply during the COVID-19 Crisis with an Innovative 3D-Printed Mask Adaptor. *Healthcare* **2020**, *8*, 225. [CrossRef]
15. Skrzypczak, N.G.; Tanikella, N.G.; Pearce, J.M. Open source high-temperature RepRap for 3-D printing heat-sterilizable PPE and other applications. *HardwareX* **2020**, *8*, e00130. [CrossRef]
16. Nicholson, K.; Henke-Adams, A.; Henke, D.M.; Kravitz, A.V.; Gay, H.A. Modified full-face snorkel mask as COVID-19 personal protective equipment: Quantitative results. *HardwareX* **2021**, *9*, e00185. [CrossRef] [PubMed]
17. Hubbard, B.R.; Pearce, J.M. Conversion of self-contained breathing apparatus mask to open source powered air-purifying particulate respirator for fire fighter COVID-19 response. *HardwareX* **2020**, *8*, e00129. [CrossRef] [PubMed]

18. Gallup, N.; Pringle, A.M.; Oberloier, S.; Tanikella, N.G.; Pearce, J.M. Parametric nasopharyngeal swab for sampling COVID-19 and other respiratory viruses: Open source design, SLA 3-D printing and UV curing system. *HardwareX* **2020**, *8*, e00135. [CrossRef] [PubMed]
19. Manoj, A.; Bhuyan, M.; Banik, S.R.; Sankar, M.R. 3D printing of nasopharyngeal swabs for COVID-19 diagnose: Past and current trends. *Mater. Today Proc.* **2020**, *44*, 1361–1368. [CrossRef]
20. Abuzairi, T.; Sumantri, N.I.; Irfan, A.; Mohamad, R.M. Infrared thermometer on the wall (iThermowall): An open source and 3-D print infrared thermometer for fever screening. *HardwareX* **2020**, *9*, e00168. [CrossRef]
21. Santhosh, R.; Yadav, S. Low Cost Multipurpose UV-C Sterilizer box for protection against COVID'19. In Proceedings of the 2021 International Conference on Artificial Intelligence and Smart Systems (ICAIS), Coimbatore, India, 25–27 March 2021; pp. 1495–1498. [CrossRef]
22. Bentancor, M.; Fernández, S.; Viera, F.; Etcheverry, S.; Poradosú, C.; D'Angelo, P.; Montemuiño, H.; Mirazo, S.; Irigoyen, Á.; Sanabria, A.; et al. LUCIA: An open source device for disinfection of N95 masks using UV-C radiation. *HardwareX* **2021**, *9*, e00181. [CrossRef]
23. Oberloier, S.; Gallup, N.; Pearce, J. Overcoming supply disruptions during pandemics by utilizing found hardware for open source gentle ventilation. *HardwareX* **2021**, *11*, e00255. [CrossRef]
24. Pearce, J.M. A review of open source ventilators for COVID-19 and future pandemics. *F1000Research* **2020**, *9*, 218. [CrossRef] [PubMed]
25. Abuzairi, T.; Irfan, A. Basari COVENT-Tester: A low-cost, open source ventilator tester. *HardwareX* **2021**, *9*, e00196. [CrossRef] [PubMed]
26. Read, R.L.; Clarke, L.; Mulligan, G. VentMon: An open source inline ventilator tester and monitor. *HardwareX* **2021**, *9*, e00195. [CrossRef]
27. Voas, J.; Kshetri, N.; DeFranco, J.F. Scarcity and Global Insecurity: The Semiconductor Shortage. *IT Prof.* **2021**, *23*, 78–82. [CrossRef]
28. Paul, S.K.; Chowdhury, P.; Chowdhury, T.; Chakrabortty, R.K.; Moktadir, A. Operational challenges during a pandemic: An investigation in the electronics industry. *Int. J. Logist. Manag.* **2021**, *34*, 336–362. [CrossRef]
29. Coughlin, T. Impact of COVID-19 on the Consumer Electronics Market. *IEEE Consum. Electron. Mag.* **2020**, *10*, 58–59. [CrossRef]
30. Wu, X.; Zhang, C.; Du, W. An Analysis on the Crisis of "Chips shortage" in Automobile Industry—Based on the Double Influence of COVID-19 and Trade Friction. *J. Phys. Conf. Ser.* **2021**, *1971*, 012100. [CrossRef]
31. Miller, F.A.; Young, S.B.; Dobrow, M.; Shojania, K.G. Vulnerability of the medical product supply chain: The wake-up call of COVID-19. *BMJ Qual. Saf.* **2020**, *30*, 331–335. [CrossRef]
32. Sajjad, A. The COVID-19 pandemic, social sustainability and global supply chain resilience: A review. *Corp. Gov. Int. J. Bus. Soc.* **2021**, *21*, 1142–1154. [CrossRef]
33. Flowers, P.F.; Reyes, C.; Ye, S.; Kim, M.J.; Wiley, B.J. 3D printing electronic components and circuits with conductive thermoplastic filament. *Addit. Manuf.* **2017**, *18*, 156–163. [CrossRef]
34. Kwok, S.W.; Goh, K.H.H.; Tan, Z.D.; Tan, S.T.M.; Tjiu, W.W.; Soh, J.Y.; Ng, Z.J.G.; Chan, Y.Z.; Hui, H.K.; Goh, K.E.J. Electrically conductive filament for 3D-printed circuits and sensors. *Appl. Mater. Today* **2017**, *9*, 167–175. [CrossRef]
35. Zhang, D.; Chi, B.; Li, B.; Gao, Z.; Du, Y.; Guo, J.; Wei, J. Fabrication of highly conductive graphene flexible circuits by 3D printing. *Synth. Met.* **2016**, *217*, 79–86. [CrossRef]
36. Zhang, S.; Wang, B.; Jiang, J.; Wu, K.; Guo, C.F.; Wu, Z. High-Fidelity Conformal Printing of 3D Liquid Alloy Circuits for Soft Electronics. *ACS Appl. Mater. Interfaces* **2019**, *11*, 7148–7156. [CrossRef]
37. Czyżewski, J.; Burzyński, P.; Gaweł, K.; Meisner, J. Rapid prototyping of electrically conductive components using 3D printing technology. *J. Mater. Process. Technol.* **2009**, *209*, 5281–5285. [CrossRef]
38. Olivas, R.; Salas, R.; Muse, D.; MacDonald, E.; Wicker, R.; Newton, M.; Church, K. Structural Electronics through Additive Manufacturing and Micro-Dispensing. *Int. Symp. Microelectron.* **2010**, *2010*, 000940–000946. [CrossRef]
39. Min, H.; Lee, B.; Jeong, S.; Lee, M. Fabrication of 10 μm-scale conductive Cu patterns by selective laser sintering of Cu complex ink. *Opt. Laser Technol.* **2017**, *88*, 128–133. [CrossRef]
40. Sigmarsson, H.H.; Kinzel, E.C.; Xu, X.; Chappell, W.J. Selective Laser Sintering of Multilayer, Multimaterial Circuit Components. In Proceedings of the 2006 IEEE MTT-S International Microwave Symposium Digest, San Francisco, CA, USA, 11–16 June 2006; pp. 1788–1791. [CrossRef]
41. Palmer, J.A.; Summers, J.L.; Davis, D.W.; Gallegos, P.L.; Chavez, B.D.; Yang, P.; Medina, F.; Wicker, R.B. Realizing 3-D Interconnected Direct Write Electronics Within Smart Stereolithography Structures. In Proceedings of the ASME 2005 International Mechanical Engineering Congress and Exposition, Orlando, FL, USA, 5–11 November 2005; pp. 287–293. [CrossRef]
42. Lopes, A.J.; MacDonald, E.; Wicker, R.B. Integrating stereolithography and direct print technologies for 3D structural electronics fabrication. *Rapid Prototyp. J.* **2012**, *18*, 129–143. [CrossRef]
43. Digi-Key Corporation. Digi-Key Company History. Available online: https://web.archive.org/web/20160416045752/https://www.digikey.com/en/resources/about-digikey (accessed on 7 July 2022).
44. Digi-Key Corporation. Embedded–Microsontrollers. Available online: https://www.digikey.ca/en/products/filter/embedded-microcontrollers/685 (accessed on 3 July 2022).
45. Selenium. Software Freedom Conservancy. 2022. Available online: https://pypi.org/project/selenium/ (accessed on 3 July 2022).
46. Beautiful Soup. Leonard Richardson. 2022. Available online: https://pypi.org/project/beautifulsoup4/ (accessed on 3 July 2022).

47. Jones, R.; Haufe, P.; Sells, E.; Iravani, P.; Olliver, V.; Palmer, C.; Bowyer, A. RepRap—The replicating rapid prototyper. *Robotica* **2011**, *29*, 177–191. [CrossRef]
48. Sells, E.; Bailard, S.; Smith, Z.; Bowyer, A.; Olliver, V. RepRap: The Replicating Rapid Prototyper: Maximizing Customizability by Breeding the Means of Production. In Proceedings of the World Conference on Mass Customization and Personalization, Cambridge, MA, USA, 7–10 October 2009; pp. 568–580. [CrossRef]
49. Bowyer, A. 3D Printing and Humanity's First Imperfect Replicator. *3D Print. Addit. Manuf.* **2014**, *1*, 4–5. [CrossRef]
50. What Is OpenSCAD? Openscad 2021.01. 2022. Available online: https://github.com/openscad/openscad (accessed on 7 July 2022).
51. FreeCAD 0.20. FreeCAD. 2022. Available online: https://github.com/FreeCAD/FreeCAD (accessed on 27 June 2022).
52. Prusa Firmware MK3. Prusa3D. 2022. Available online: https://github.com/prusa3d/Prusa-Firmware (accessed on 27 June 2022).
53. PrusaSlicer. Prusa3D. 2022. Available online: https://github.com/prusa3d/PrusaSlicer (accessed on 27 June 2022).
54. Open Science Foundation. Additive Manufacture Breakout Board. Available online: https://osf.io/dh6uy/ (accessed on 11 July 2022).
55. LondonHydro, "Hydro One". Available online: https://www.hydroone.com:443/rates-and-billing/rates-and-charges/electricity-pricing-and-costs (accessed on 7 July 2022).
56. Wittbrodt, B.T.; Glover, A.G.; Laureto, J.; Anzalone, G.C.; Oppliger, D.; Irwin, J.L.; Pearce, J.M. Life-cycle economic analysis of distributed manufacturing with open-source 3-D printers. *Mechatronics* **2013**, *23*, 713–726. [CrossRef]
57. Wittbrodt, B.; Pearce, J.M. The effects of PLA color on material properties of 3-D printed components. *Addit. Manuf.* **2015**, *8*, 110–116. [CrossRef]
58. Woern, A.L.; McCaslin, J.R.; Pringle, A.M.; Pearce, J.M. RepRapable Recyclebot: Open source 3-D printable extruder for converting plastic to 3-D printing filament. *HardwareX* **2018**, *4*, e00026. [CrossRef]
59. Alexandre, A.; Sanchez, F.A.C.; Boudaoud, H.; Camargo, M.; Pearce, J.M. Mechanical Properties of Direct Waste Printing of Polylactic Acid with Universal Pellets Extruder: Comparison to Fused Filament Fabrication on Open-Source Desktop Three-Dimensional Printers. *3D Print. Addit. Manuf.* **2020**, *7*, 237–247. [CrossRef]
60. Cruz Sanchez, F.A.; Boudaoud, H.; Hoppe, S.; Camargo, M. Polymer recycling in an open-source additive manufacturing context: Mechanical issues. *Addit. Manuf.* **2017**, *17*, 87–105. [CrossRef]
61. Sanchez, F.A.C.; Boudaoud, H.; Camargo, M.; Pearce, J.M. Plastic recycling in additive manufacturing: A systematic literature review and opportunities for the circular economy. *J. Clean. Prod.* **2020**, *264*, 121602. [CrossRef]
62. King, D.L.; Babasola, A.; Rozario, J.; Pearce, J. Mobile Open-Source Solar-Powered 3-D Printers for Distributed Manufacturing in Off-Grid Communities. *Chall. Sustain.* **2014**, *2*, 18–27. [CrossRef]
63. Wong, J.Y. Ultra-Portable Solar-Powered 3D Printers for Onsite Manufacturing of Medical Resources. *Aerosp. Med. Hum. Perform.* **2015**, *86*, 830–834. [CrossRef]
64. Gwamuri, J.; Franco, D.; Khan, K.Y.; Gauchia, L.; Pearce, J.M. High-Efficiency Solar-Powered 3-D Printers for Sustainable Development. *Machines* **2016**, *4*, 3. [CrossRef]
65. Mohammed, M.I.; Wilson, D.; Gomez-Kervin, E.; Vidler, C.; Rosson, L.; Long, J. The Recycling of E-Waste ABS Plastics by Melt Extrusion and 3D Printing Using Solar Powered Devices as a Transformative Tool for Humanitarian Aid. In Proceedings of the 2018 International Solid Freeform Fabrication Symposium, Austin, TX, USA, 13–15 August 2018. [CrossRef]
66. Zhong, S.; Pearce, J.M. Tightening the loop on the circular economy: Coupled distributed recycling and manufacturing with recyclebot and RepRap 3-D printing. *Resour. Conserv. Recycl.* **2017**, *128*, 48–58. [CrossRef]
67. Oellermann, M.; Jolles, J.W.; Ortiz, D.; Seabra, R.; Wenzel, T.; Wilson, H.; Tanner, R. Harnessing the Benefits of Open Electronics in Science. *arXiv* **2021**, arXiv:2106.15852.
68. Baden, T.; Chagas, A.M.; Gage, G.; Marzullo, T.; Prieto-Godino, L.L.; Euler, T. Open Labware: 3-D Printing Your Own Lab Equipment. *PLoS Biol.* **2015**, *13*, e1002086. [CrossRef] [PubMed]
69. Pearce, J.M. *Open-Source Lab: How to Build Your Own Hardware and Reduce Research Costs*; Elsevier: Amsterdam, The Netherlands, 2013.
70. Chagas, A.M. Haves and have nots must find a better way: The case for open scientific hardware. *PLoS Biol.* **2018**, *16*, e3000014. [CrossRef] [PubMed]